03 Jun 1993, 2:00 pm - 4:00 pm

Failures of Quay Walls During Chilean Earthquake of March 1985

P. Ortigosa
University of Chile, Santiago de Chile

E. Retamal
University of Chile, Santiago de Chile

R. V. Whitman
Massachusetts Institute of Technology, Cambridge, Massachusetts

Proceedings: Third International Conference on Case Histories in Geotechnical Engineering, St. Louis, Missouri, June 1-4, 1993, Paper No. 3.10

Failures of Quay Walls during Chilean Earthquake of March 1985

P. Ortigosa
Professor of Civil Engineering, IDIEM, University of Chile, Santiago de Chile

R. V. Whitman
Professor of Civil Engineering, Massachusetts Institute of Technology, Massachusetts

E. Retamal
Professor of Civil Engineering, IDIEM, University of Chile, Santiago de Chile

SYNOPSIS Extensive damage took place in the quay walls in the Ports of Valparaíso and San Antonio during the Chilean earthquake of March 1985. Different types of retaining structures such as gravity retaining walls built with concrete blocks, sheetpiles and decks on vertical piles were subjected to large shaking ranging from 0.3 - 0.45g at Valparaíso Port to more than 0.6g at San Antonio. Some of the retaining structures collapsed and others behave quite well. In addition, some liquefaction and settlements in the sandy fill below the yards did occur at San Antonio, along with permanent displacements in the fill slope behind some of the decks supported by piles. The behavior of 7 berths at Valparaíso and 7 berths at San Antonio is discussed taking into account soil characteristics and field measurements performed after the earthquake.

INTRODUCTION

The Chilean earthquake of March 3, 1985, became one of the most significant, well recorded, and major earthquake to date. The main earthquake occurred at 19.47 hours local time. Figure 1 shows the general area affected by the earthquake, which included San Antonio, Valparaíso, the metropolitan region and Santiago, and many surrounding cities. Significant ground motions were recorded for a relatively long duration. Seismological records indicate that the earthquake actually consisted of two main shocks occurring within 11 seconds of each other as shown in Fig. 1, with surface wave magnitude of 5.2 and 7.8, respectively.

Peak ground acceleration (PGA) values recorded by strong motion accelerometers of the Chilean instrumentation network in the area most affected by the earthquake were reported by Saragoni (1986). The maximum recorded PGA value was 0.67g for the N10E component at Llolleo, about 4.5 km south of San Antonio.

An intensity of VII on the modified Mercalli scale was generally applicable in the coastal area between the cities of Valparaíso and San Antonio (near the central zone of the energy release). However, in the city and port of San Antonio intensity was rated as 8.5

THE PORT OF VALPARAISO

The port of Valparaíso along with the port of San Antonio are the two major ports that function as a gateway of the Santiago metropolitan area. Figure 2 shows the port of Valparaíso, built during 1913 - 1924 using gravity quay walls of concrete blocks without shear keys. The typical cross section at berths 1 to 5 is illustrated in Fig. 3; Fig. 4 shows the pier's cross section.

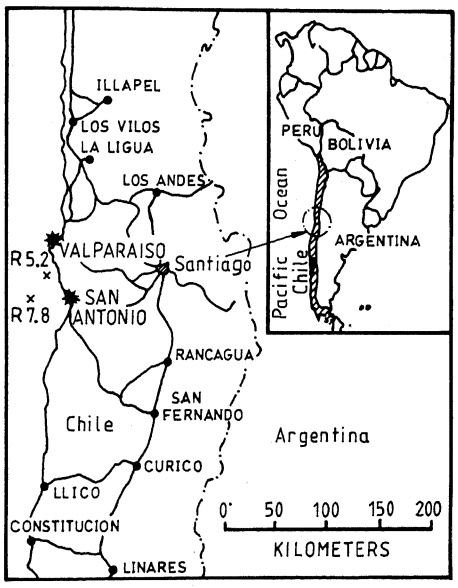

Fig. 1 General Area of the Earthquake.

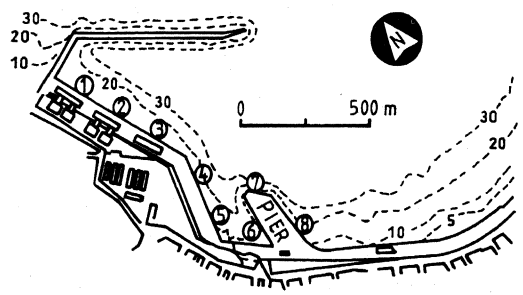

Fig. 2 Port of Valparaíso and Berth Locations.

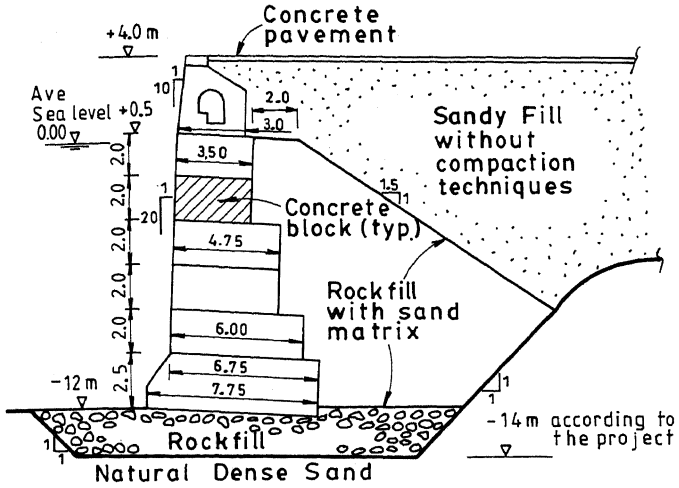

Fig. 3 Valparaíso: Typical Cross Section at Berth 1 to 5.

Main failures in the quay walls were characterized by permanent horizontal displacements due to sliding between concrete blocks at a depth of about 12m below the yard surface. By using earth pressures given by the Mononobe and Okabe method, even with an inverted seismic pressure triangle, the critical failure mechanism was found to be a rigid body sliding at a depth of 12 m, which checks with the observed behaviour (Ortigosa et al, 1986). However, in berth 5, having the poorest soil conditions as shown in Fig. 5, a permanent rigid body rotation at the wall base was measured. Additionally, borings performed through the concrete wall at berths 3 and 5 found a thickness of the rockfill below the wall between 1.5 to 2.1m at berth 3 and only 0.8m at berth 5. Therefore, the combination at berth of the poorest soil conditions along wi maximum contact pressures at the foundati level (over 10 kg/cm^2) would explain th rotational mechanism. A summary of t horizontal displacements at the top of the qu walls is illustrated in Fig. 6.

Permanent horizontal displacements along the ya surface were obtained by measuring crack open ings in the concrete pavement. The horizont displacement patterns in berths 1 to 5 a presented in Fig. 7; figure 4 shows the patte in the pier. The horizontal displaceme attenuation with increasing distance from t retainning wall defines a sliding wedge with slope of about 1:2 (V:H) in all the berths. Th finding is at least qualitatively consistent wi analytical studies showing a flatter wedge ang for an active seismic condition than for a stat active condition.

Peak Ground Acceleration

Unfortunately no instruments were installed the port and therefore no ground accelerati records are available. However, the PGA w estimated using the horizontal permanent displ cements, δ_H, measured in those quay walls wi sliding mechanism. This enables use of t simplified formula given by Richards and El (1979) based in the Newmark rigid block concep along with the use of a seismic thrust giv by the Mononobe - Okabe formula:

$$\delta_H = 0.087 \frac{V^2_{max}}{a_{max} \cdot g} \left[\frac{a_{max}}{C_{crit}}\right]^4$$

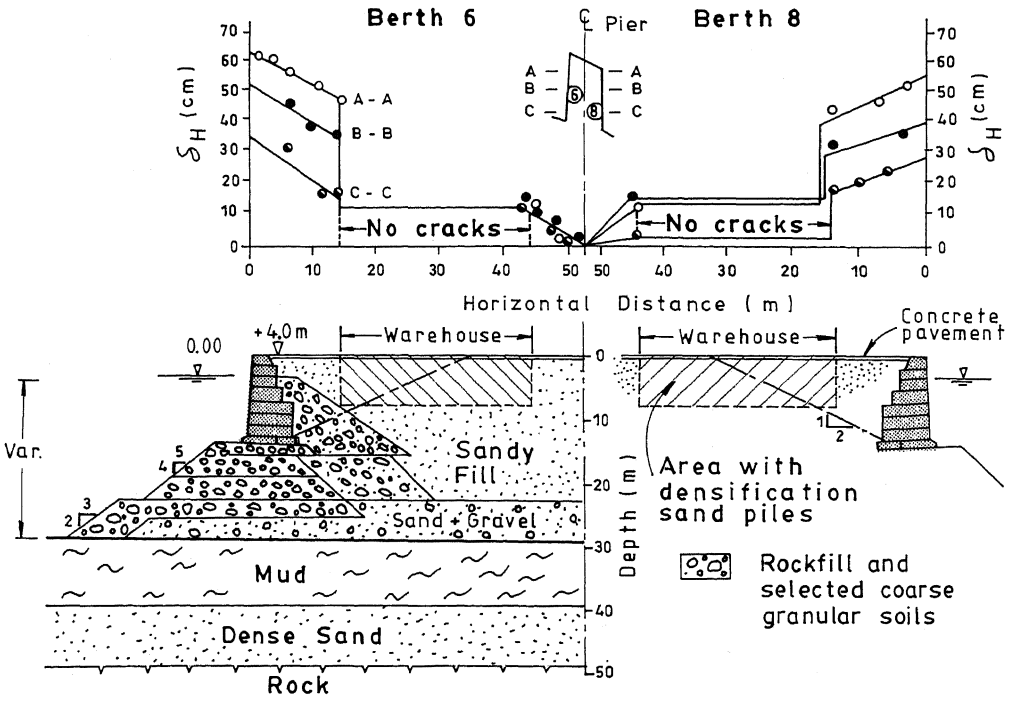

Fig. 4 Valparaíso: Pier Cross Section and Horizontal Displacements on the Yard Surface.

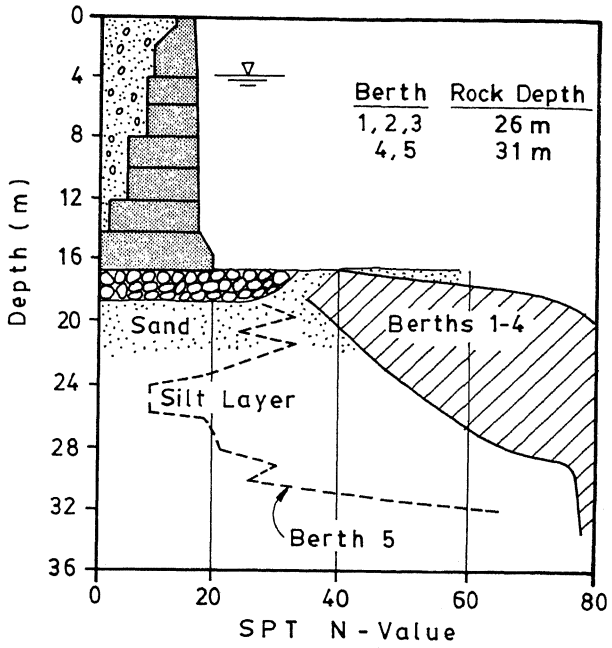

Fig. 5 Valparaíso: Foundation Soil Conditions at Berths 1 to 5.

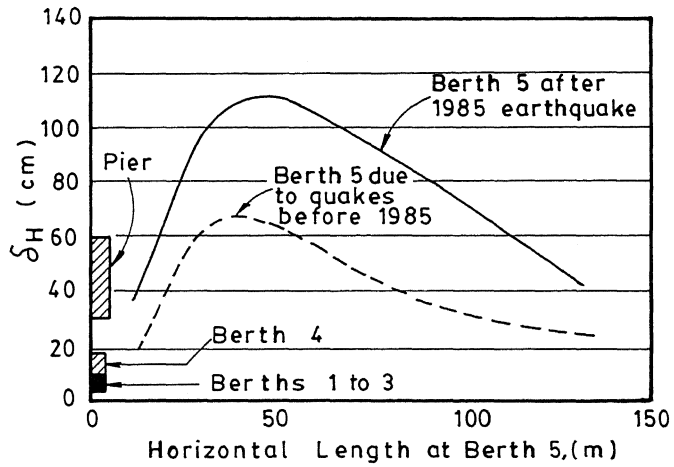

Fig. 6 Valparaíso: Seismic Horizontal Displacements at the Top of the Quay Walls.

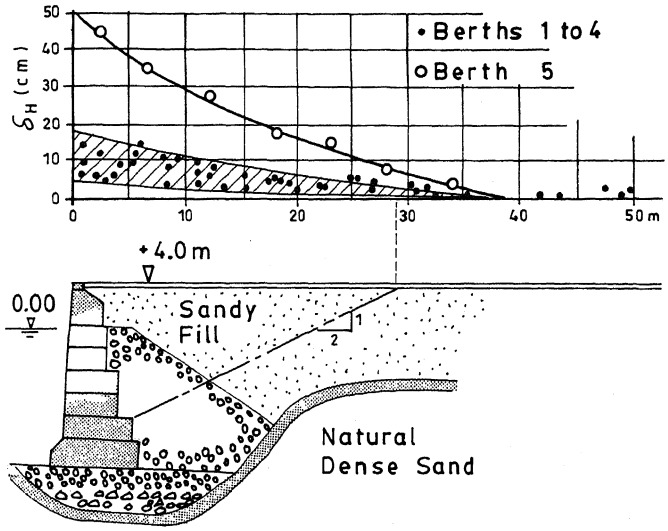

Fig. 7 Valparaíso: Seismic Horizontal Displacements on the Yard Surface.

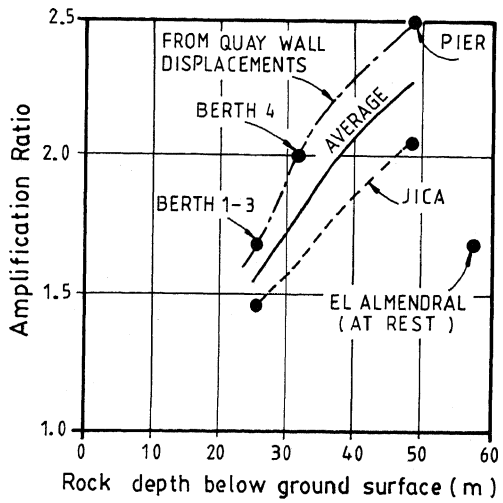

Fig. 8 Valparaíso: Acceleration Amplification Ratio.

where g = acceleration of gravity (cm/sec^2); δ_H = permanent horizontal displacement of the wall (cm); a_{max} = peak ground acceleration (g's); V_{max} = peak ground velocity (cm/sec) and C_{crit} = threshold ground acceleration (g's) that triggers the sliding mechanism. By defining $V_{max} = C\ a_{max}$, eq. (1) gives:

$$a_{max} = 6.46 \frac{1}{(C)^{0.4}} (C_{crit})^{0.8} (\delta_H)^{0.2} \qquad (2)$$

From the processed acceleration records given by Saez and Holmberg (1991), an average C value equal 70cm/sec was obtained. A threshold acceleration C_{crit} = 0.12g was reported by Ortigosa et al (1986) for the critical sliding surface, assuming a seismic pore pressure ratio r_u = 40% in the retained soil and using the Mononobe - Okabe seismic thrust computed with a measured angle of friction of 40°. The 40% pore pressure ratio was just an estimation, based on no evidence of liquefaction on the yard surfaces. (For r_u = 0 a value of C_{crit} = 0.16g is obtained, which in eq.2 gives peak ground acceleration 25% greater).

By replacing C = 70cm/seg, C_{crit} = 0.12g and the average wall horizontal displacements measured at each berth, it was possible to compute a_{max} by means of equation (2).

The peak ground accelerations were devided by the peak acceleration a_{rmax} = 0.18g recorded in a sound granitic rock outcrop 3km away from the port (Saragoni, 1986). The amplification ratio defined as a_{max}/a_{rmax} was consequently obtained on those berths with sliding mechanism as shown

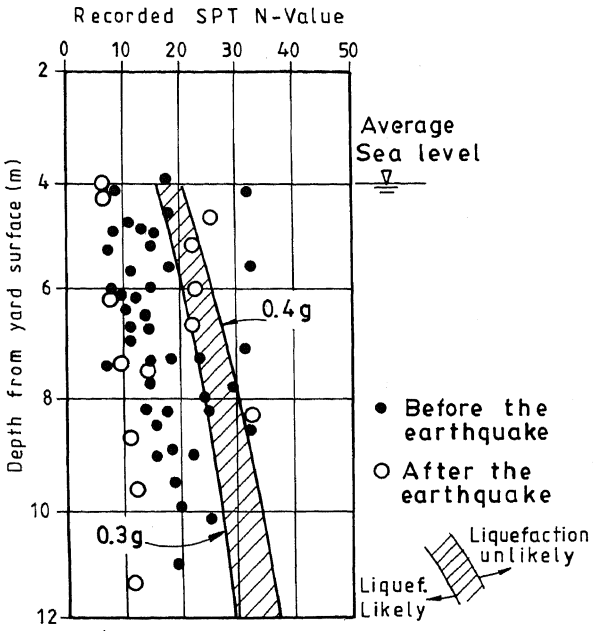

Fig. 9 Valparaíso: Critical Liquefaction Range for the Sandy Fill.

in Fig. 8. This figure includes amplification ratios reported by the Japan International Cooperation Agency (JICA, 1985 - 1986) obtained by means of one-dimensional amplification analysis using the computer program SHAKE.

A comparison with the acceleration amplification ratio at El Almendral site, located about 2km from the port area, is included in Fig. 8. This ratio was computed with the PGA recorded at that site, which is an at rest deposit with a 3.5m artificial fill resting on dense sands. Differences in the amplification ratios as compared with the El Almendral at rest deposit, can be explained by the "topographic" effects introduced by the quay wall discontinuities and the pier embankment.

Liquefaction analysis

Liquefaction analysis for the sandy fill behind the retaining walls was conducted based on the procedure outlined by Seed et al. (1983) for an earthquake M = 7.8 Richter, and the results are presented in Fig. 9. Critical envelopes were defined using a PGA range obtained with the average curve in Fig. 8, unit weights of 1.9ton/m^3 and 2.1ton/m^3 over and below the water table, respectively, an average D_{50} = 0.40mm (ranges between 0.2 to 0.8mm) and an average non-plastic fines content of 10% (ranges between 2 to 20%). The SPT in Chile has an energy ratio of 60% and, therefore, the final step to determine the critical envelopes in terms of recorded SPT-N values was based on c_n, which is a correction coefficient to normalize N-values for an overburden pressure of 1kg/cm^2. Results in Fig. 9 show a tendency to liquefaction, but no evidence of such phenomenon was observed.

THE PORT OF SAN ANTONIO

Figure 10 shows berth locations in the port of San Antonio. Quay walls at berths 1 and 2 were built in 1918 using concrete blocks similar to those used in the port of Valparaíso. Berths 3 and 4 are anchoraged sheetpile walls built just before 1985 and in the second half of the 1960 decade, respectively. Berth 5 is a deck on vertical piles started during 1975 and berths 6 and 7 are decks built during 1913-1918.

In all berths the fill was poured over the seabed without special compaction techniques. Fill characteristics change from one berth to other, ranging from non-plastic fine sands to rockfills. Below the fills, dense non-plastic fine sands and hard clays were detected, reaching an average depth of 26 m below the yard surfaces. At this depth a dense sandy gravel was detected reaching at least 50 m below the sea bed (JICA, 1985-1986).

The recorded SPT N-Values are summarized in Fig. 11. Values for the fill deposit do not include those records influenced by boulders and high gravel contents. As shown in Fig. 11, thicker sandy fills were detected at berths 1 to 3 where extensive damage took place during the earthquake.

The undrained shear strength of the hard clay, S_u, was measured by means of unconfined compression tests and CIU triaxial tests on undisturbed samples. Results from triaxial tests are summarized in Fig. 12, which shows the normalized undrained strength as a function of the effective isotropic confining pressure, σ'_c. Most of the samples exhibited a plastic failure.

Berths behavior along the Pier

The cross section at berth 4 is shown in Fig. 13. Due to a good quality fill behind the sheetpile, only minor displacements were detected in the yard surface.

Figure 14 shows the typical cross section in berth 5 and the location of 6 topographic control points. Taking as a reference level the deck surface where displacements were negligible, it was possible to compute the average vertical strain, ε_s, due to the seismic densification of the granular fill, using topographic data from seven sections along the berth:

$$\varepsilon_{s1} = \frac{\rho_1}{H} \times 100\ (\%) \qquad (3)$$

$$\Delta\varepsilon_s = \frac{\rho_2 - \rho_T}{H} \times 100\ (\%) \qquad (4)$$

$$\varepsilon_{sT} = r_N\, \varepsilon_{s1} \qquad (5)$$

$$\varepsilon_{s2} = \Delta\varepsilon_s + \varepsilon_{sT} \qquad (6)$$

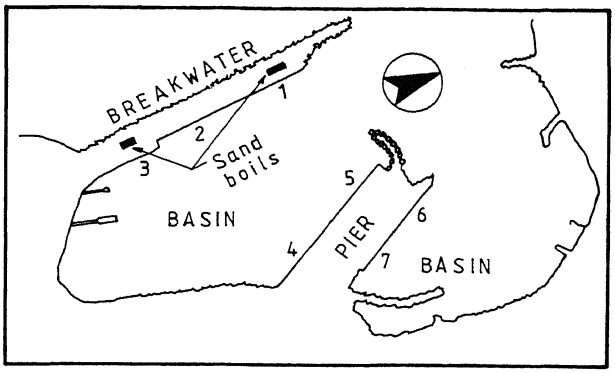

ig.10 Port of San Antonio and Berth Locations.

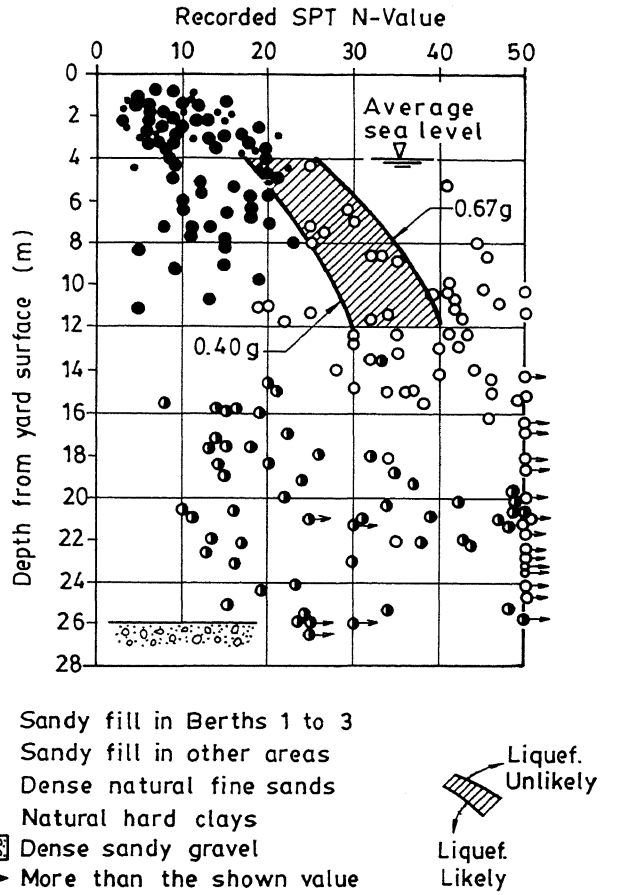

ig.11 San Antonio: Recorded Standard Penetration Values.

quation (3) gives the average seismic vertical train at point 1 where vertical settlements anged between 30 to 60cm with a typical value of 0cm. Lack of topographic levels before the arthquake at points 2 and T located at greater istances from the deck, made impossible a direct omputation of the vertical strain at those oints. Therefore, an indirect procedure was sed to compute the average seismic vertical train at point 2:

- The differential vertical strain between points 2 and T was computed using eq.(4) by introducing the measured settlements ρ_2 and ρ_T referred to the deck.

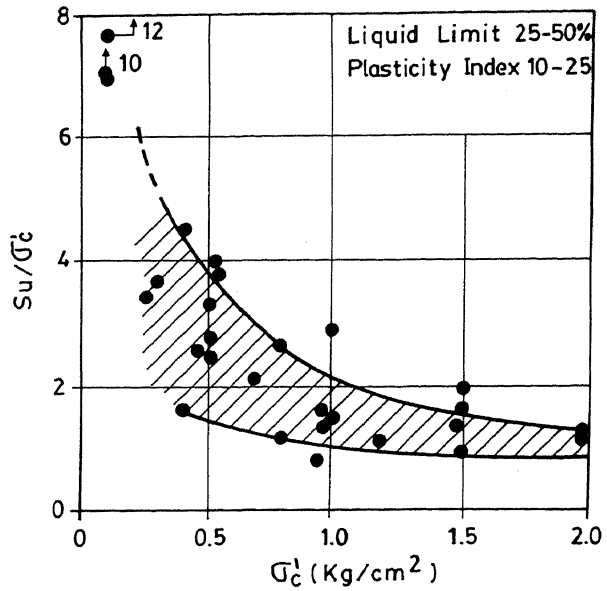

Fig.12 San Antonio: Undrained Shear Strength at 10% strain for the Hard Clay.

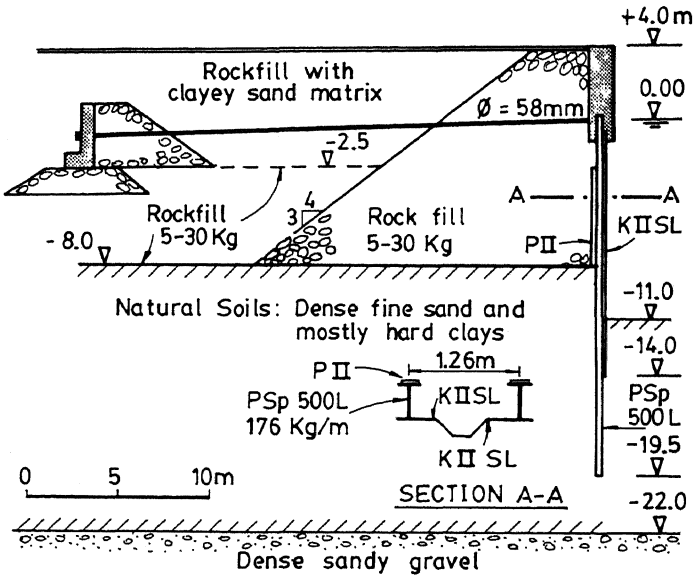

Fig.13 San Antonio: Cross Section at Berth 4.

- By means of equation (5) the strain at point T (old fill) was computed, using as a reference value the seismic average strain measured at point 1 (new fill). On doing this a reduction coefficient $r_N = 0.25$ was introduced. This coefficient represents the additional densification due to an earthquake acting in an old granular soil, which has been subjected to previous earthquakes (for example the 1971 earthquake with M = 7.5 Richter). Values of r_N for N = 30 additional cycles were obtained from drained cyclic triaxial tests reported on different rockfill materials (Hamed, 1992).

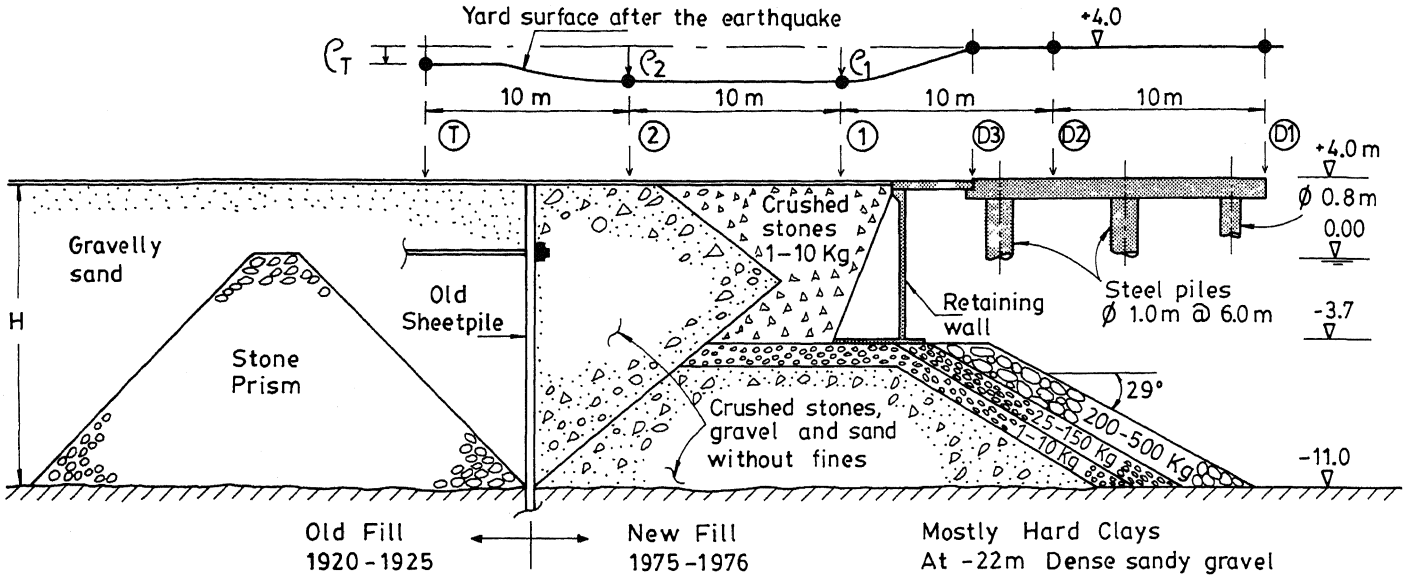

Fig.14 San Antonio: Cross Section at Berth 5.

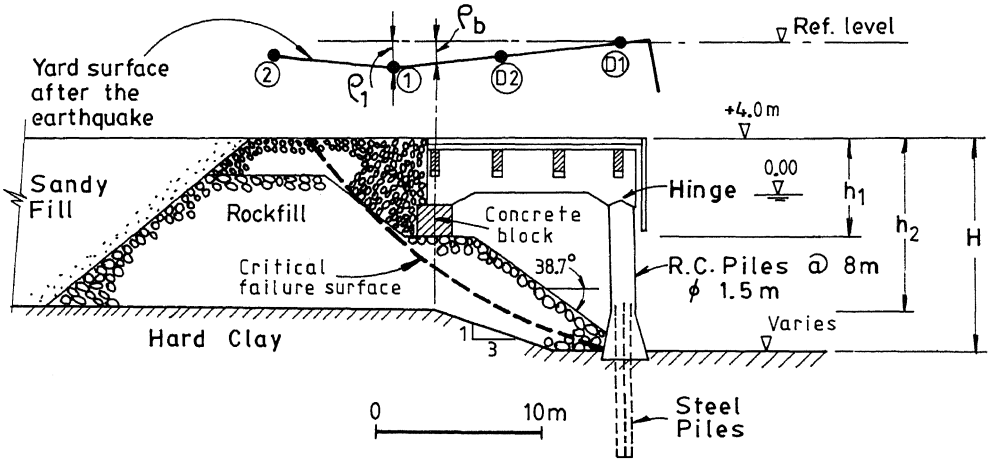

Fig.15 San Antonio: Cross Section at Berths 6 and 7.

- The seismic vertical strain at point 2 was computed using eq.(6).

Similar values of about 3% were obtained at points 1 and 2 (new fill). The strain at point T (old fill) was 0.8%, which is quite similar to the 1% average seismic strain obtained in the old fills at berths 6 and 7 as will be discussed in the analysis of berths 6 and 7. Finally, it is necessary to point out that eq.(3) was used assuming small displacements in the embankment slope. As a matter of fact, slope permanent displacements were computed in the range 2.5 - 5cm using the procedure outlined in the analysis of berths 6 and 7.

The typical cross section at berths 6 and 7 is shown in Fig. 15. Sixteen sections along those berths were surveyed after the earthquake by means of 4 control points per section, ending with a typical settlement pattern as shown in Fig. 15. This pattern suggests a deck rotation as a rigid body due to permanent seismic displacements in the embankment slope. This behaviour was considered by the project in 1913 by introducing a hinged support between the deck and the reinforced concrete piles. In order to assess the permanent average displacement, $\bar{s}$, due to seismic sliding along a critical failure surface in the embankment slope, the following simplified equations were used:

$$\bar{s} = \frac{s_1 + s_b}{2} \tag{7}$$

$$s_1 = \frac{\rho_1 - \varepsilon_s h_2}{\cos\alpha_1} \tag{8}$$

$$s_b = \frac{\rho_b - \varepsilon_s (h_2 - h_1)}{\cos\alpha_b} \quad (9)$$

$$\varepsilon_s \approx \frac{\rho_1 - \rho_b}{h_1} \quad (10)$$

Equation (7) gives the average slope displacement as a function of the permanent dispacements at point 1, s_1, and at the middle of the concrete block, s_b, which are the only two points where it was possible to assess values from the topographic measurements. In order to substract the seismic permanent displacements due to the rockfill densification, ε_s, eqs.(8) and (9) were used. In this equations α_1 and α_b are the angles between the vertical and the tangent to the critical failure surface at verticals through point 1 and the middle of the concrete block. Results obtained from slope stability analysis using a rockfill angle of internal friction ranging 38° - 43° gives pairs α_1, α_b in the range 45 - 60°. Fortunately, the average $\bar{s}$ values were more or less the same in spite of using different α_1, α_b pairs. Finally, eq.(10) gives the average vertical densification strain in the rockfill. Computed ε_s values at the 16 sections along berths 6 and 7 varies from 0.6% to 1.6% with an average of 1%. This strain corresponds to an old fill and is similar to the 0.8% obtained in the old fill at berth 5.

Figure 16 illustrates the slope permanent displacements normalized by a reference displacement, $\bar{s}_o$, the value at a section with a total height H = 13m. Both $\bar{s}$ and $\bar{s}_o$ were obtained by means of eqs.(7) through (9) using ε_s = 1%. These empirical results are compared with predicted values using charts for dry granular soils given by Musante (1979) using the Newmark rigid block approach and artificial Chilean earthquake records. Predicted normalized values in Fig. 16 are independent of the maximum horizontal acceleration in the slope of the embankment, a_{max}, and they are almost independent of the rockfill angle of internal friction, ϕ.

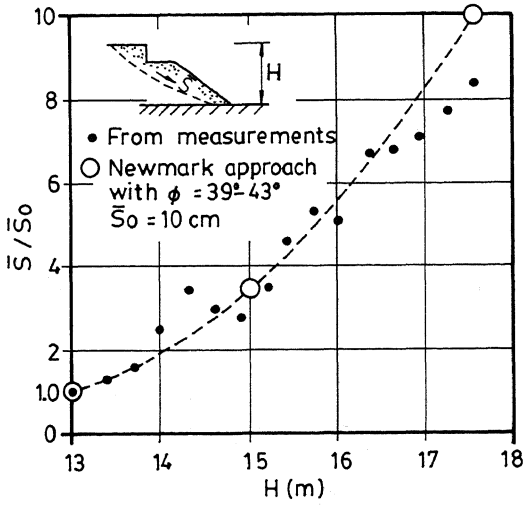

Fig.16 San Antonio: Normalized Slope Permanent Displacements in Berths 6 and 7.

Values of a_{max} vs ϕ were computed to match $\bar{s}$ values obtained with the dashed curve in Fig. 16. This was accomplished using Musante charts and introducing a correction factor to take into account the effect of the rockfill bouyancy (i.e. inertia forces were computed using 25% of water as part of the rockfill skeleton, which gives an equivalent total unit weight of $1.7\gamma_b$, where γ_b is the bouyant unit weight of the rockfill). On the other hand, the frictional shear forces along the critical sliding surface are proportional to γ_b. Therefore, actual maximum accelerations were amplified by a factor equals to 1.7. By considering $V_{max} = C\, a_{max}$ (see eq.1) permanent displacements using the Newmark approach are proportional to $(a_{max})^5$, so permanent displacements using Musante charts for dry soils were amplified by $(1.7)^5$ to take into account the rockfill bouyancy.

Using an average normal effective stress on the critical failure surface equal to 0.5kg/cm^2 and laboratory failure envelopes at large strains reported by Hamed (1992) on different rockfills tested with homotetic gradations, the friction angle ranges from 50 to 55° (includes cohesion intercept). On the other hand, using Fig. 17 with a_{max} = 0.45g (minimum value reported by JICA, 1985-1986) and the PGA = 0.67g recorded at the Llolleo station, the backfigured angles of friction in the rockfill ranges between 42.5° - 44°, which are about 10° below friction angles measured in the laboratory. This difference could be explained by the vertical acceleration component which reached a peak value of 0.85g at the Llolleo station.

Berths behavior along the Breakwater

The typical section at berths 1 and 2 before the 1985 earthquake is shown in Fig. 18. This figure indicates a wall rotation due to previous earthquakes ranging 3° to 6°, which can be explained by simple stability analysis using the Mononobe - Okabe formula. For an angle of 3° the analysis shows a threshold horizontal acceleration of the order of 0.08g to trigger a rotation failure, even without introducing seismic pore pressures in the retained soils. During the 1985

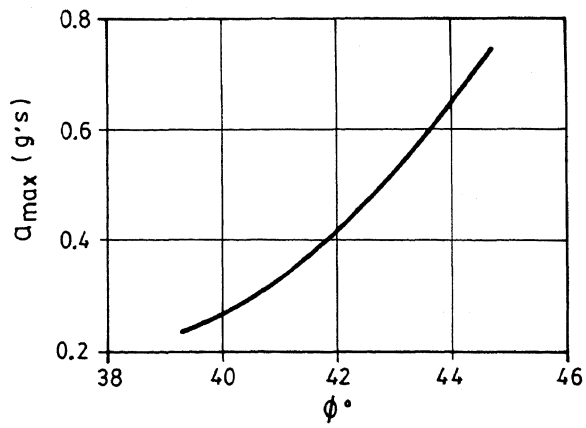

Fig.17 San Antonio: Peak Acceleration vs. Rockfill Angle of Friction to match Permanent Slope Displacements in Berths 6 and 7.

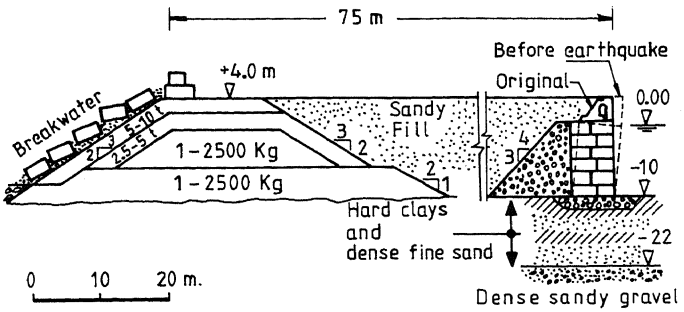

Fig.18 San Antonio: Cross Section at Berths 1 and 2.

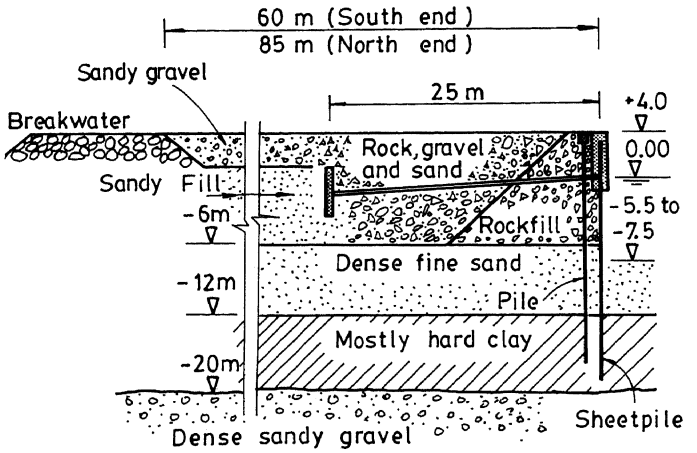

Fig.19 San Antonio: Cross Section at Berth 3.

earthquake peak accelerations were much greater than 0.08g, so the wall collapse at berth 2 was not a surprise. The retaining wall at berth 1 did not collapse, but rotated as a rigid body reaching an angle of 25° at the south end of the berth and 10° to 13° in most of the berth length. This behaviour could be explained by considering the plastic permanent strains in the clay layers below the wall base. Location and thickness of the clay layers shown in the soil profiles are in accordance with this hypothesis. Unfortunately, there is a lack of data concerning to the rockfill thickness below the wall. As a matter of fact, only two borings at berth 1 give rockfill thickness between 3 to 5 m. At berth 2 thicker clay layers and a thinner rockfill support could explain the collapse.

Bearing capacity analysis using the upper limit of the undrained clay strength in Fig. 12 gives a failure stress at the foundation level of the order of 16kg/cm^2, which is less than the 30kg/cm^2 maximum working stress computed with the threshold acceleration 0.08g. When considering the effect of the rockfill and the dense sand layers, failure stress increases. However, earthquake accelerations were much greater than 0.08 g, which means an exponential increase of the working stress. Hence, failure of the foundation clayey soils arises as the most probable mechanism for explaining the rotational mechanism in berths 1 and 2.

The cross section at berth 3 is shown in Fig. 19. Tie rods have a diameter of 65mm, a yield stress of 45kg/mm^2 and a rupture strength of 70kg/mm^2. The sheetpile wall has a flexural modulus of 4550cm^3/m, a yield stress of 40kg/mm^2 and a rupture strength of 55kg/mm^2.

At the time of the earthquake the dredged level was 3.5 to 5.5m above the final operation level. However, seaward deformations of the copeline were between 55 to 120cm. Post earthquake inspections showed a lack of tension in the tie rods, suggesting a seaward displacement of the segmented deadman beam. Actually, tie rods exhibited a curvature with horizontal and vertical maximum displacements, measured from the theoretical straight line, up to 50cm and the segments of the deadman beam tilted vertically and horizontally with angles up to 4.5°. This behavior could be attributed to construction defects along with liquefaction of the sandy fill behind the beam. Whichever is the reason, the sheetpile wall moved seaward due to earth pressures under a cantilever condition. To reach the sheetpile yield stress the threshold acceleration computed using $\phi = 38°$ for the fill material and the Mononobe and Okabe formula ranged from 0.15 to 0.25g depending on using an inverted or normal triangle to represent the seismic earth pressure distribution. Actual soil accelerations were greater than 0.25g, which means that yield stresses were reached in the sheetpile wall.

If a total liquefaction condition is considered in the coarse granular fill between the sheetpile and the deadman, a sustained working stress in the sheetpile somewhat bigger than 7000kg/cm^2 is obtained, so a collapse condition would be reached or tie rods would be in tension. Consequentely, it is difficult to envision that a total liquefaction occured in the fill behind the sheetpile wall, specially when considering the coarse grain composition of that fill.

Only two small areas over sandy fills exhibited sand boils emerging through joints in the concrete slabs at the yard surface. One of this areas was located about 10m behind the deadman at berth 3 (approximately 5m^3 of fine sand emerged) and the other in the bottom of a coal deposit 25 x 80m in plant and 3m deep, located at berth 1 (approximately 15m^3 of fine sand and silts emerged). Other areas over sandy fills at berth 2 seem to have liquefied, when looking at large foundation distortions, suggesting bearing capacity failures.

The liquefaction analysis was performed under the same basis used at the port of Valparaíso and results are shown in Fig. 11. Critical envelopes were defined using a PGA range with an upper limit equals to the PGA recorded at Llolleo station, unit weights of 1.7ton/m^3 and 2.0ton/m^3 over and below the water table, respectively, an average $D_{50} \approx 0.15$mm (ranges between 0.12 to 0.25mm) and an average non-plastic fines content of 10% (ranges between 2 to 22%). Results on Fig. 11 clearly suggests liquefaction for the sandy fills, but this phenomenon is not well defined for the dense natural sand deposits where dilatancy would preclude liquefaction. There-

fore, results in Fig. 11 confirm liquefaction evidences detected on those areas with sandy fills poured over the sea bottom without compaction techniques. Finally, it is interesting to point out that sandy fills were old deposits, subjected to previous earthquakes such as the 1971 earthquake with M = 7.5 Richter. This previous earthquakes seems to have precluded a more extensive liquefaction.

As regards to seismic settlements, no confident topographic references were available prior to the earthquake. Besides, seawards movements of the retaining structures make difficult to asses settlements due to seismic densification. In spite of those difficulties, Poran et al (1989) present results of seismic densification in the sandy fill along the breakwater.

CONCLUSIONS

The variety of waterfront structures at Valparaiso and San Antonio experienced a wide rage of behavior in response to the very strong shaking during the 1985 Chile earthquake. While important information concerning pre-earthquake conditions often were not available, it has been possible to make informative and useful comparisons between observations and behavior that might have been expected.

Gravity walls experienced permanent outward displacements. Where foundation conditions were good, displacements resulting from sliding between the blocks composing the walls and were small - a few inches. These displacements were quite similar to those predicted by sliding block theory. With poor foundation conditions, there was tilting and actual overturning. Liquefaction, or at least pore pressure increase, contributed to the forces causing movement and overturning, although it may not have been the dominant factor. In general, there was less evidence of liquefaction than would have been expected from measured standard penetration resistances.

One anchored bulkhead at San Antonio performed very well, with only small outward movements that did not interfere with continued use. This case is a clear demonstration that anchored bulkheads can be constructed to resist extremely strong shaking, if suitable backfill is used and proper attention given to anchorage. A second bulkhead experienced movement of nearly a meter, apparently because of inadequate anchorage.

A newly-constructed pile-supported deck performed well, although settlements occurred in the adjacent filled area. The magnitude of these settlements varied from about 1% to about 3%, in accordance with predictions based upon laboratory tests. There were significant movements of the slope of rock fill beneath another pile-supported deck. The friction angle, needed to explain the magnitude of these movements using conventional sliding block analysis, was less than expected. It is possible that vertical ground accelerations were the reason for the actual movements.

ACKNOWLEDGEMENT

The writers wish to acknowledge the financial support offered by the US National Science Foundation and our appreciation for the valuable data provided by Empresa Portuaria de Chile, the Port Departament of the Chile Ministry of Public Works and by Mr. Gustavo Dahlgren.

REFERENCES

Hamed, J. (1992). "Análisis Comparativo de Escorias de Acería y Enrocado de Canteras", Memoria para optar al título de Ingeniero Civil, Universidad de Chile.

JICA, Japan International Cooperation Agency (1985-1986). "Report on Damage to Port Facilities in the Port of Valparaíso by the Earthquake on March 3, 1985", April 1985; and "Study on the Development of the Ports of Valparaíso and San Antonio in the Republic of Chile", Interim Report, Feb. 1986 and Final Report, August 1986.

Musante, H. (1979). "Estabilidad Sísmica de Taludes Arenosos, Método Simplificado", Revista del IDIEM, Universidad de Chile, Sept.

Ortigosa, P., Retamal E., Acevedo, P. and Hidalgo, E. (1986). "Aspectos Geotécnicos en los Malecones de los Puertos de Valparaíso y San Antonio", 4as Jornadas Chilenas de Sismología e Ingeniería Antisísmica, Viña del Mar.

Poran, C.J., Greenstein J. and Berger, L. (1989). "Earthquake - induced Settlements in Port Facilities in Chile", Proc.XII Int. Conference on Soil Mechanics and Found. Eng., Vol.3, Río de Janeiro, Brazil.

Richards, R. Jr. and Elms, D.G. (1979). "Seismic Behavior of Gravity Retaining Walls", Jour. of the Geotech. Engineering Div., ASCE, April.

Saragoni, R. (1986). "Análisis de los Acelerogramas del Terremoto del 3 de Marzo, 1985", El Sismo del 3 de Marzo 1985 - Chile, Ed. Acero Comercial S.A. y Universidad de Chile.

Seed, H.B., Idriss, I.M. and Arango, I. (1983). "Evaluation of Liquefaction Potential Using Field Performance Data", Jour. of the Geotech. Engineering Division, ASCE, March.

Saez, A. y Holmberg, A. (1991). "Análisis de los Acelerogramas del Terremoto de Chile de 1985", Memoria para optar al título de Ingeniero Civil, Universidad de Chile.